Alqalam Journal of Medical and Applied Sciences. 2026;9(11):3860-3869
https://doi.org/10.54361/ajmas.261144

Original article

Development of Graphene-Modified Rubberized Asphalt Mixtures for Enhanced Rutting Resistance and Extended Pavement Life in Extreme High Temperatures: A Case Study

Makari A. Makari

Department of Architectural Engineering, Higher Institute of Sciences and Technology-Mezda, Libya
Email. Makari.ahmed92@gmail.com

Abstract
In such conditions, asphalt pavements have to deal with various challenges, such as elevated pavement temperature, high axle loads, oxidation, and tough construction conditions. This study aims to explore the possibilities for improving the performance of crumb-rubber-modified asphalt for southern Libyan roads using graphene nanoplatelets (GNPs). For this purpose, the sample set includes six different compositions of binders: control without any modifications; asphalt-rubber binder with 18% crumb rubber; binder with 0.1% GNPs without rubber; and three composites of asphalt-rubber binder with 18% crumb rubber and 0.1%, 0.3%, and 0.5% of GNPs, respectively. Assessment involves application of DSR, MSCR, BBR, Hamburg wheel tracking, RLFN, and MS tests, as well as reporting of known parameters describing cracking response. Among the selected sample set, the mixture with 18% crumb rubber and 0.3% GNPs (M4) was identified as the most promising in terms of high-temperature performance. Compared with the control mixture, it demonstrates 3.15 times lower non-recoverable creep compliance at 3.2 kPa (from 8.65 kPa^{-1} to 3.15 kPa^{-1}), or a 63.6% reduction of the initial value. The value of Hamburg rutting depth at 70°C has decreased from 11.8 to 4.0 mm, whereas the number of flow has increased from 192 to 742 cycles. However, recalculated values of stress sensitivity of the MSCR test exceeded 75% for all samples tested, and therefore the possibility of compliance with specification requirements cannot be stated unconditionally. Exploratory service-life and economic estimates point to potentially advantageous properties, but both their attribution to certain composition and environmental impact should be verified based on the original model files and life-cycle inventories.
Keywords: Graphene Nanoplatelets; Crumb Rubber; Modified Asphalt; Rutting Resistance; Desert Pavements.

Introduction

Permanent deformation is one of the main problems encountered by asphalt pavements subjected to high service temperatures and heavy loads. As temperature increases, the sensitivity of the binder to viscous flow increases, which, in turn, leads to a reduction in the ability of the aggregate-binder combination to resist accumulated shearing deformation. This results in depression on the wheel track that leads to degradation of riding qualities, increased maintenance requirements, and reduced traffic safety. Graphene modifiers have attracted considerable attention because of their structural characteristics, properties of interaction with the binder, and their reinforcing abilities that allow to change the rheological properties of the binder. Nevertheless, the effect is dependent on modifier type, dispersion, filling amount, and binder properties. Moreover, long-term characteristics and transfer of laboratory improvements into real life are of key importance [1] .The Southern region of Libya is an appropriate environment for the application of asphalt pavement, which should work under the influence of intense solar radiation, wide temperature fluctuations, and heavy cargo loading. In the original study, the maximum pavement surface temperatures in selected highways were about 78–82°C. The figures are used without any verification against the climatic data.

The rationale behind modifying graphene is that graphene is able to control molecular mobility depending on temperature and to improve the load-carrying properties of the binder by means of reinforcing structures. Indeed, experimental studies have proved that the addition of graphene increases the stiffness and elasticity of binders, but their effect and the nature of such an effect depend greatly on the amount used and particle network formation. Therefore, the results achieved using a high dose of graphene cannot be used when considering low-dose GNP modifications[2]. In any case, there are reasons for further research at the mixture level. There have been studies reporting positive changes in the wheel tracking resistance and indirect tensile strength, among others, after adding graphene platelets into penetration grade 60/70 asphalt. But it would be wrong to assume that the dosage providing good results in one system can also provide good results in another system [3]. So, the use of GNPs in combination with crumb rubber might be promising because crumb rubber provides a deformable polymeric phase, and graphene platelets can reinforce the binder matrix and increase interfacial stability. But the efficiency of such a mixture has to be estimated according to workability, moisture resistance, cracking resistance, and processability.

Research problem and contribution

The research question is not limited to how much the graphene improves binder stiffness. It asks if a practically applicable graphene-rubber mixture can improve the material's ability to resist permanent deformation without producing stress sensitivity, compaction problems, extensive processing demands, and reduced crack resistance. The originality of the manuscript lies in an organized analysis of the binder and mixture dataset available and the correction of internal numerical inconsistencies as well as the distinction between laboratory measurements and theoretical applications.

Copyright *Author (s) 2026. Distributed under Creative Commons CC BY 4.0*
Received*: 17-09-2026 -* ***Accepted****: 15-11-2026 -* ***Published****: 23-11-2026*

Research objectives

Goals of the experiment:

1. Investigate rheological and mechanical properties of unmodified, rubber-modified, graphene-modified, and graphene-rubber composite formulations.
2. Establish the right concentration of graphene nanoplatelets (GNPs) in the series of rubberized formulations under study.
3. See if any improvements in binder characteristics translate into mixture performance in terms of resistance to rutting.
4. Evaluate performance implications of moisture susceptibility and low-temperature stiffness.

Literature Review

Recent studies have focused on testing the incorporation of graphene into rubber-modified asphalt for tires. The results obtained include higher rutting indices and better elastic recovery, lower irrecoverable creep compliance, better fatigue properties, and higher resistance to phase separation. This confirms that the area of graphene-rubber modification is one of the proven research directions; therefore, novelty can be defined through the specific materials, exposure conditions, and verification process [4]. Not all GNP grades are equal as materials. The platelet diameter, platelet thickness, platelet surface characteristics, and platelet tendency to agglomerate affect their interactions with asphalt. Recent research has found that GNP grades with a larger platelet diameter have a greater effect on the high-temperature rheology than the smaller GNP grades. This stresses the importance of using the properties of the supplied GNP grades rather than the monolayer graphene properties as references[5]. The dispersion of the nanoparticles is also very important. An increase in GNP grade amount does not necessarily mean that there will be a corresponding increase in performance.

Graphene oxide (GO) consists of oxygen-containing functional groups and shows chemical dissimilarities to comparatively unfunctionalized graphene nanoplatelets (GNPs). Studies on GO-rubber composite-modified asphalt showed better rheological characteristics and reduced segregation, with physical compatibility predominantly being the main modification mechanism found. Such studies prove the validity of the composite-modification hypothesis, but do not provide an independent proof of the same mechanisms in the case of GNPs[6] .

The 2026 paper found that 0.3% GO is an optimal amount in its own rubber-modified asphalt system, improving the asphalt in terms of high-temperature characteristics, aging, and storage stability. While such an amount matches the candidate dosage mentioned above, it cannot be considered a direct confirmation due to the differences in chemistry of the modifiers, rubber content, binders, and preparation conditions [7]. The environmental benefits go well beyond simply having the presence of the recycled rubber. The assessment process is affected by the modifier production, transport, temperature during mixing, processing energy, construction, maintenance frequency, and lifespan of the paving material. Studies that have been conducted on the comparison of rubberized warm-mix asphalt recently have done so in light of construction and maintenance processes, showing that assumptions about durability and system boundaries can significantly influence the level of environmental benefits estimated. [8]

Research gap

The justification for the research gap is the inclusion of locally available materials from Libya, exposure to extreme temperatures, advanced testing of binders and mixtures, and local calibration of performance. However, there is no existing evidence supporting a clear-cut statement on the lack of similar studies in existence. This study aims to fill in the need for a replicable test using locally available information.

Methods

Study framework and data status

The research is organized into three layers, including characterization of the materials, lab testing, and application testing.

Application corridors

Three corridors were identified in the original study framework.

Table 1. Reported application corridors and exposure conditions.

Corridor	Reported maximum surface temperature	Reported ESAL value*	Principal concern
Sabha–Murzuq	82°C	8.5×10^6	Rutting under substantial freight loading
Ubari–Ghat	78°C	3.2×10^6	Combined thermal and moisture-related deterioration
Al-Qatrun–Niger border	80°C	12.8×10^6	Severe axle loading and permanent deformation

These values "ESALs (2025)" represent annual loading or cumulative design traffic.

Copyright *Author (s) 2026. Distributed under Creative Commons CC BY 4.0*
Received*: 17-09-2026 -* ***Accepted****: 15-11-2026 -* ***Published****: 23-11-2026*

Constituent materials

Base asphalt binder

The reported base binder was penetration grade 60/70 asphalt obtained from the Zawiya refinery.

Table 2. Reported properties of the base binder.

Property	Test designation	Reported value
Penetration at 25°C	ASTM D5	65 × 0.1 mm
Softening point	ASTM D36	49.5°C
Rotational viscosity at 135°C	ASTM D4402	0.42 Pa·s
Specific gravity	ASTM D70	1.025
Flash point	ASTM D92	285°C

Aggregate

The base binder used for the project is penetration-grade asphalt with designation 60/70 obtained from Zawiya refinery. The final material characterization should identify the distinction between the coarse and fine aggregate fractions, including specifications for the aggregate grading, mineral filler characteristics, and other volume-related characteristics.

Table 3. Reported aggregate properties.

Property	Test designation	Reported value
Los Angeles abrasion loss	ASTM C131	22%
SSD specific gravity	ASTM C127	2.68
Water absorption	ASTM C127	1.8%
Polished stone value	BS 812-114	52

Crumb rubber

In the case of crumb rubber presented above, its production was carried out using scrap tire rubber, wherein the crumb size falls within 0.425 mm to 0.600 mm, textile content is lower than 0.4%, and metal content is less than 0.1%. The crumb size should not be indicated merely as No. 40 since it covers several sieve openings.

Graphene nanoplatelets

The provided properties of the graphene nanoplatelets (GNPs) include: purity higher than 99%, average thickness from 1 to 3 nm, lateral size from 5 to 10 μm, specific surface area from 400 to 500 m^2/g, and density close to 2.2 g/cm^3. These properties must be validated by the corresponding certificate of analysis of a particular batch of the material. The theoretical surface area value that corresponds to the ideal monolayer graphene cannot be considered instead of real properties of the nanoplatelets.

Formulation matrix and dosage basis

There are six substances in the formulation table instead of five. The IDs are always maintained in the modified analysis.

Table 4. Formulation matrix.

Formulation	Base asphalt, mass parts	Crumb rubber, mass parts*	GNPs, mass parts*	Description
M0	100	0	0	Unmodified control
M1	100	18	0	Rubber-modified asphalt
M2	100	0	0.1	GNP-modified asphalt
M3	100	18	0.1	Rubber–GNP composite
M4	100	18	0.3	Rubber–GNP composite
M5	100	18	0.5	Rubber–GNP composite

To be interpreted consistently, these values are stated as additions on 100 mass parts of base asphalt.

Binder preparation and experimental controls

Preparation procedure is documented to have included heating the base asphalt to 170°C, mixing with crumb rubber using high-shear stirring at 3000 rpm for 45 min, mixing the sample further with the GNP dispersion for 30 min and sonication of the mixture for 15 min. The GNP material needs to be described as dispersed in the medium and not dissolved.

The suggested ratio of 1:5 between GNP and carrier oil is a very important experimental parameter. In terms of weight, if this ratio is considered, then 0.1%, 0.3%, and 0.5% of GNP will be equivalent to approximately 0.5%, 1.5%, and 2.5% carrier oil to the base asphalt, respectively. Carrier oil may affect viscosity, stiffness and cracking behavior; hence, its inclusion calls for oil-matched controls. The final method must include specifications about the geometry of the mixer used, mass of the batch, ultrasonication energy and power, temperature control and holding period.

Copyright *Author (s) 2026. Distributed under Creative Commons CC BY 4.0*
Received: *17-09-2026 -* ***Accepted:*** *15-11-2026 -* ***Published:*** *23-11-2026*

https://doi.org/10.54361/ajmas.261144

Mixture design and specimen preparation

In the initial design approach, the nominal maximum aggregate size used was 19 mm, and the Superpave gyratory compaction test was conducted with an initial design effort of 75 gyrations. Design effort needs to be justified with respect to the traffic anticipated and the specifications applicable.

The stated nominal binder content is 5.2% by mass of aggregates. If the above figure is considered for the complete modified binder, the equivalent percentage by mass of the total mixture would be:

$$P_b = \frac{0.052}{1 + 0.052} \times 100 = 4.94\%.$$

The final document must state whether the binder content includes rubber, GNPs, and carrier oil. Though a standard binder content in all the samples may ease comparison, it does not necessarily show that each sample was optimized. Thus, for each formula, the following must be stated: air voids, mineral aggregate voids, voids occupied by asphalt, effective binder content, and density.

Performance testing

Multiple stress creep and recovery

MSCR assessment includes creep compliance irrecoverably and recovery at 0.1 and 3.2 kPa. The stress sensitivity is described by:

$$J_{nr,\text{diff}} = \frac{J_{nr,3.2} - J_{nr,0.1}}{J_{nr,0.1}} \times 100.$$

Compliance assessment must use the appropriate test temperature, conditioning procedure, and traffic designation. A decrease in $J_{nr,3.2}$ alone does not establish conformity with AASHTO M 332. [9]

Dynamic shear and low-temperature testing

The supplied program includes DSR temperature sweeps and BBR testing after appropriate aging. Performance grading requires the complete set of applicable criteria rather than isolated values of $G*/sin\delta$ or stiffness. The grading interpretation must also preserve the distinction between test temperature and nominal low-temperature grade. [10]

Mixture-level testing

The components of the mix design program being researched include the Hamburg wheel-tracking test performed at 50°C and 70°C, repeated-load flow number test performed at 50°C, susceptibility to moisture test, and IDEAL-CT test performed at 25°C. The 70°C condition in the Hamburg test will be considered a high-temperature research condition. The last methodology needs to define the geometry of specimens, conditioning procedure, loading procedure, cessation criterion, and loading repetitions, either in wheel passes or full cycles. The connection of IDEAL-CT with ASTM D8225 instead of AASHTO TP105 needs to be considered. The focus on instruments and data processing needs to be emphasized since the difference in instruments and data registration may affect the cracking resistance index. [11]

Results

High-temperature rheological response

In all cases, there is a reduction in the rutting parameter with an increase in the temperature level. Among the different formulations, M4 shows the maximum value, while M5 and M3 come next in order. At 76°C, the percent increases from M0 are 27.5%, 43.8%, 85.0%, 115.0%, and 97.5% for M1, M2, M3, M4, and M5 respectively. As a result, the initial assumption regarding the maximum response of M3 is inconsistent with the results in the table. Thus, the transition from M4 to M5 is associated with a decrease in the effect of GNP at the maximum dose. The possible reasons for such a trend may be related to the issues of agglomeration and workability. However, this cannot be confirmed with additional tests. The original grading is changed. In case the table reflects data for RTFO-aged asphalt binders, the values in the table do not confirm the stated grades according to the common aged binder criterion.

Table 5. Supplied $G*/sin\delta$ values after RTFO aging.

Formulation	64°C, kPa	76°C, kPa	82°C, kPa
M0	1.42	0.80	0.48
M1	1.75	1.02	0.65
M2	1.88	1.15	0.73
M3	2.28	1.48	1.02
M4	2.58	1.72	1.22
M5	2.42	1.58	1.10

Copyright *Author (s) 2026. Distributed under Creative Commons CC BY 4.0*
Received: *17-09-2026 -* ***Accepted:*** *15-11-2026 -* ***Published:*** *23-11-2026*

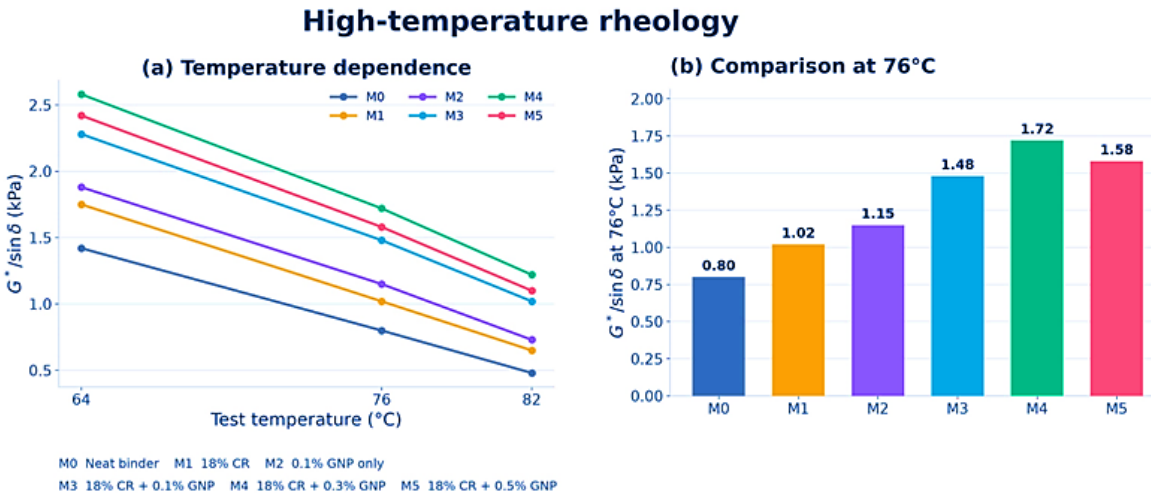

Figure 1. Relationship between temperature and the values given for rheology and comparison done at 76°C. There are no performance levels given in the figure.

MSCR response and corrected stress sensitivity

M4 exhibits the lowest compliance and highest recovery at both stress levels. Its reduction in $J_{nr,3.2}$ relative to M0 is:

$$\frac{8.65 - 3.15}{8.65} \times 100 = 63.6\%.$$

The percentage for M3 is 56.6%. It must be noted that the percentages apply to different formulations and cannot be mixed. Stress sensitivity values have a different meaning now. M4:

$$J_{nr,\,\text{diff}} = \frac{3.15 - 1.12}{1.12} \times 100 = 181.25\%.$$

All six new values are greater than 75%, signifying better performance of the composite binders in terms of compliance and recovery. Nonetheless, these do not confirm the initial claim regarding acceptable stress sensitivity. Furthermore, the test temperature during MSCR was not stated, thus making the evaluation process incomplete.

Table 6. Supplied MSCR parameters and recalculated stress sensitivity.

Formulation	$J_{nr,0.1}$, kPa^{-1}	$J_{nr,3.2}$, kPa^{-1}	$R_{,0.1}$,%	$R_{,3.2}$,%	Recalculated $J_{nr,diff}$, %
M0	2.92	8.65	31.8	17.5	196.2
M1	2.22	6.45	44.5	27.2	190.5
M2	1.92	5.12	51.2	34.5	166.7
M3	1.25	3.75	67.2	50.8	200.0
M4	1.12	3.15	71.5	56.8	181.3
M5	1.28	3.95	64.5	46.5	208.6

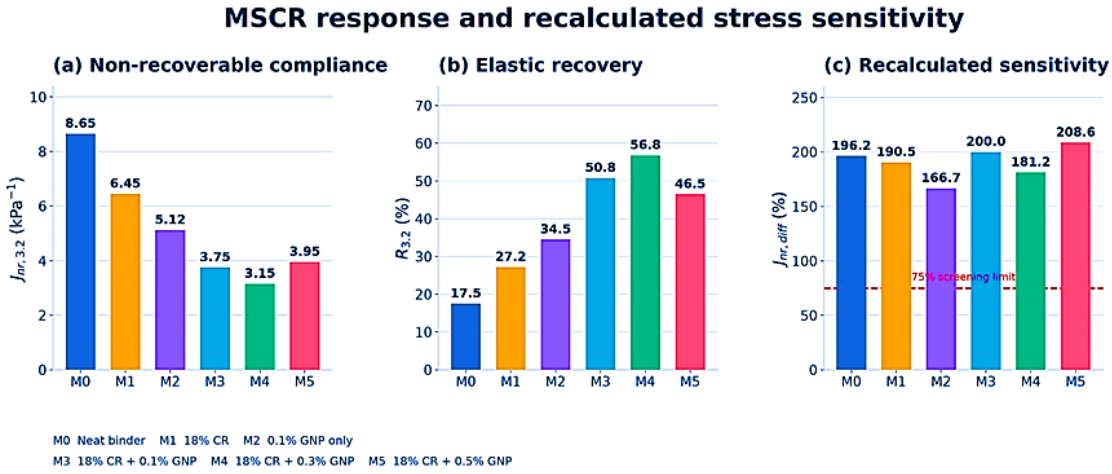

Figure 2. *Figure shows non-recoverable compliance, recoverability, and resensitized stress level. The dotted line is the 75% screening level.*

Low-temperature binder behavior

The lowest stiffness is observed in M1, at both temperatures, and thus the low-temperature effect of the rubber component is desirable for this data set. The highest GNP content in the rubberized group corresponds to higher stiffness, especially

Copyright *Author (s) 2026. Distributed under Creative Commons CC BY 4.0*
Received*: 17-09-2026 -* ***Accepted****: 15-11-2026 -* ***Published****: 23-11-2026*

for the 0.5 wt% content level. At −24°C, samples M2, M4, and M5 have stiffness values higher than 300 MPa. The reported m-values are all higher than 0.300.

Table 7. Supplied BBR results after PAV aging.

Formulation	*S* at −18°C, MPa	*m* at −18°C	*S* at −24°C, MPa	*m* at −24°C
M0	218	0.382	288	0.338
M1	198	0.408	268	0.365
M2	228	0.375	302	0.332
M3	212	0.395	282	0.352
M4	222	0.382	295	0.340
M5	235	0.370	315	0.325

Hamburg wheel tracking

The dataset *itself does not indicate whether these values are stripping inflection points, stripping criteria, or stopping conditions. At 70°C, M4 lowers the terminal rut depth by:*

$$\frac{11.8 - 4.0}{11.8} \times 100 = 66.1\%.$$

M3 results in a 61.9% reduction. Thus, both samples give good numerical results compared to the control sample, with M4 giving better results. These end-point measurements cannot give us the complete deformation processes. The time-dependent wheel tracking measurements, the density of specimens, and the point of stripping are needed for this purpose.

Table 8. Supplied Hamburg wheel-tracking results.

Formulation	Rut depth at 50°C, mm	Rut depth at 70°C, mm	Reported stripping-related repetitions at 50°C*
M0	7.2	11.8	12,200
M1	5.5	8.2	15,500
M2	5.0	7.0	16,000
M3	3.0	4.5	>20,000
M4	2.7	4.0	>20,000
M5	3.4	5.8	18,200

Repeated-load flow number

The specimen M4 possesses the maximum flow number and minimum axial strain. The flow number for M4 is about 3.86 times greater than M0's, equating to an increase of 286.5%. The consistency in rankings by Hamburg and flow number further confirms the descriptive findings on higher resistance against permanent deformation. However, the criterion "FN > 0.5," which cannot be used because of dimensionally incompatible measurements by the flow number in loading cycles, is not retained.

Table 9. Supplied repeated-load deformation results at 50°C.

Formulation	Flow number, cycles	Axial strain at 10,000 cycles, με
M0	192	2,780
M1	335	1,620
M2	442	1,250
M3	705	765
M4	742	705
M5	648	875

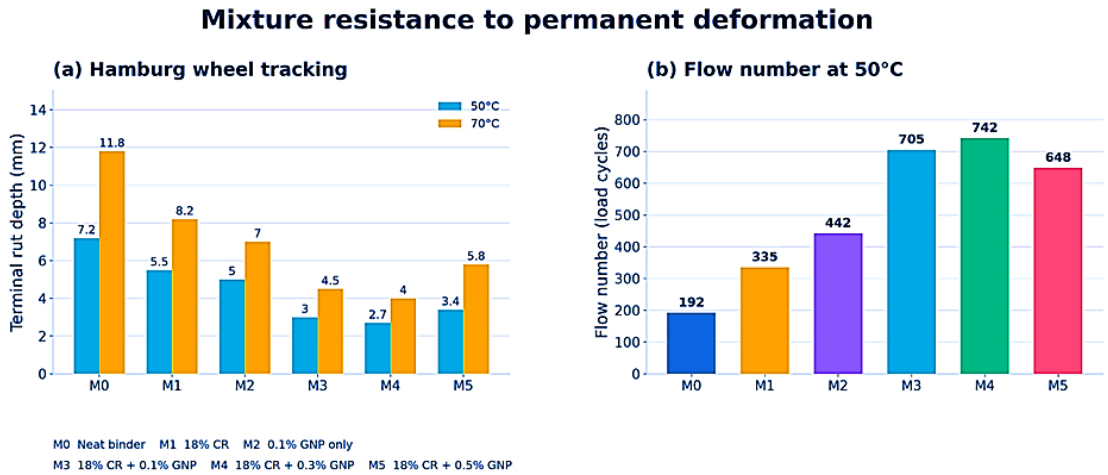

Figure 3. *Rut depths for Hamburg at 50°C and 70°C, plus flow numbers under repeated loads determined at 50°C.*

Copyright *Author (s) 2026. Distributed under Creative Commons CC BY 4.0*
Received: *17-09-2026 -* ***Accepted:*** *15-11-2026 -* ***Published:*** *23-11-2026*

https://doi.org/10.54361/ajmas.261144

Moisture susceptibility

Recalculation of TSR was done using the tensile strengths that were observed.

$$TSR = \frac{ITS_{\text{conditioned}}}{ITS_{\text{unconditioned}}} \times 100.$$

The TSR of M3 is the largest among all other alternatives, followed by that of M4. The value of TSR of M4 is 7.03 percent higher than the value of TSR of M0. Alternative M2 is marginal because the value of TSR for alternative M2 is 79.96%. This value will be rounded off to 80.0% based on standard rules of rounding.

Table 10. Recalculated tensile strength ratios.

Formulation	Conditioned ITS, kPa	Unconditioned ITS, kPa	Calculated TSR, %
M0	778	1,018	76.42
M1	888	1,078	82.37
M2	838	1,048	79.96
M3	918	1,098	83.61
M4	908	1,088	83.46
M5	868	1,068	81.27

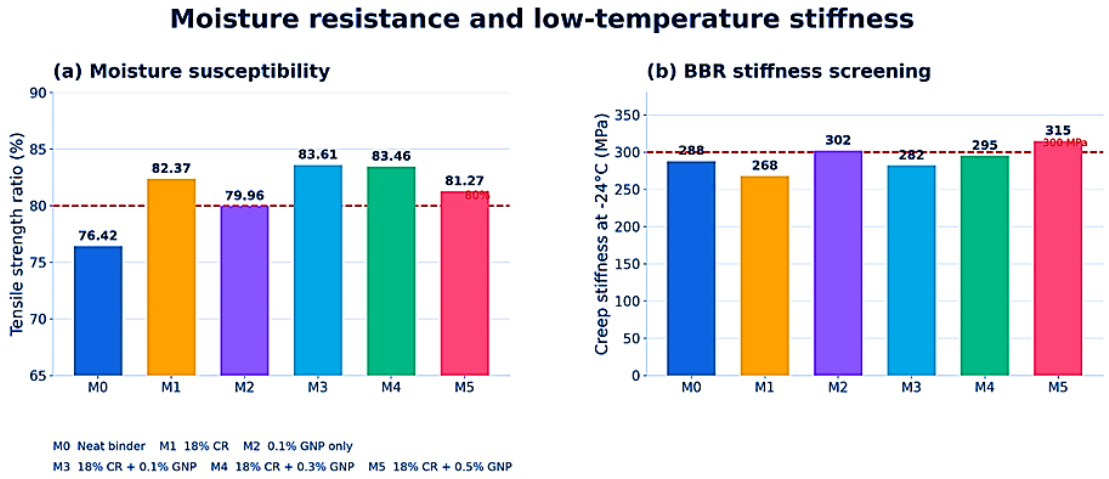

Figure 4. Thermodynamic Stress Ratio (TSR) recalculated and stiffness of BBR at −24°C are provided. Limitations of the screening process are indicated for guidance only and should not be used as a replacement for a complete specification assessment.

Reported cracking-response indicators

values in Table 11 is described as "CT Index (1/mm)" in the manuscript. Its calculation, scale, and units need to be verified before it can be considered a valid cracking tolerance index according to ASTM D8225. Based on the ranking provided, M4 is preferred over M3. But the values presented here can only be considered preliminary indications until the load-displacement curve, fracture energy values, size of specimens, and post-peak method are known. Just having a larger peak load is not enough evidence of better cracking tolerance, since post-peak energy needs to be considered.

Table 11. Supplied cracking-test outputs

Formulation	Peak load, kN	Post-peak slope magnitude, kN/mm	Reported cracking indicator*
M0	8.0	0.88	0.50
M1	9.3	0.45	0.82
M2	8.6	0.75	0.56
M3	10.0	0.40	0.90
M4	10.3	0.37	0.96
M5	9.6	0.50	0.76

Copyright *Author (s) 2026. Distributed under Creative Commons CC BY 4.0*
Received*: 17-09-2026 -* ***Accepted****: 15-11-2026 -* ***Published****: 23-11-2026*

https://doi.org/10.54361/ajmas.261144

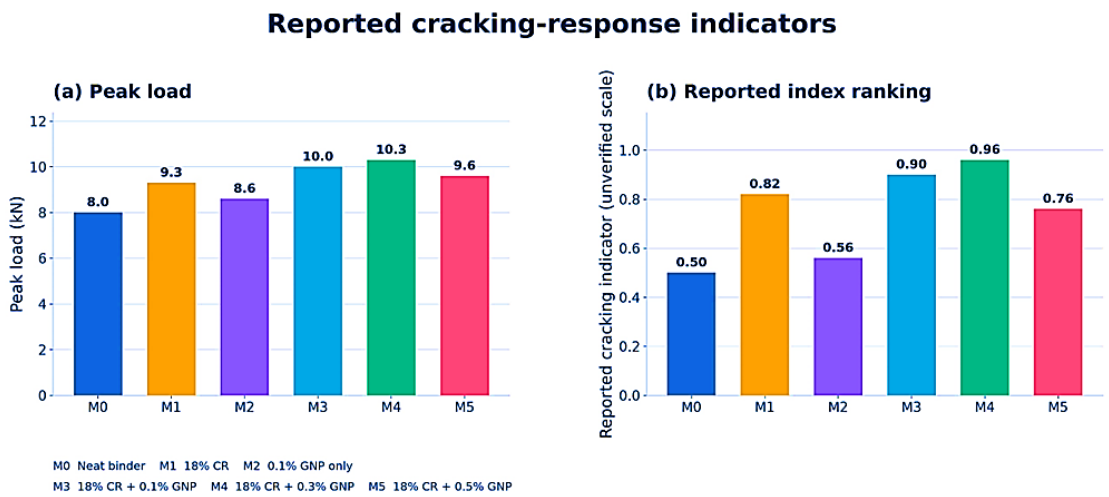

Figure 5. Peak-load data and observed indications of cracks are provided. No crack-acceptance category can be implied.

Microstructural interpretation

This is because the dispersion of the graphene nanoplatelets (GNPs) is homogeneously distributed at an intermediate dose, but agglomeration occurs at the maximum dose. In addition, FTIR intensity change does not solely determine the creation of new bonds. This increase in signals in the carbonyl area may indicate oxidation, and the π-π interaction and van der Waals force do not form covalent bonds. Thus, the proposed theory will have to remain tentative in the sense that dispersed GNPs may reinforce the binder and interact with it, but excess doses may reduce its effectiveness. The inclusion of Raman spectroscopy and quantitative microscopy along with normalized FTIR will help bolster the argument.

Candidate dosage and limits of inference

In the rubber compounds tested, the compound M4 provides the best numerical combination of rheological properties at elevated temperatures, MSCR behavior, Hamburg rut depth, and flow number. Therefore, the data allow the conclusion that a rubber compound containing **18% ground tire rubber and 0.3% GNPs is an acceptable one to be considered.**

Application Assessment for Southern Libyan Roads

Climate and traffic characterization

The surface temperature of pavements cannot be taken as being equal to the temperature used for binder design. The analysis of a locally justified temperature regime requires histories of temperatures of the pavement depth, reliability, and the effect of air temperature, solar irradiation, wind, the properties of the pavement, and traffic loads. The traffic conditions to be considered must include axle-load spectra, overloading, vehicle class, speed, lane use, and cumulative loading over a predetermined design life. These considerations are particularly necessary because a material that behaves well under laboratory rutting tests may still have poor performance if other aspects are not good enough.

Exploratory pavement-performance scenario

From age 6.5 to age 11.2, there is an observed change of 72.3%, whereas the claimed reduction in the frequency of rutting is 65.5%.

Table 12. Reported, unverified pavement-performance scenario.

Output	Baseline	Modified alternative*
Reported annual rutting rate, mm/year	2.9	1.0
Bottom-up fatigue-related time, years	8.2	13.8
Top-down cracking-related time, years	6.0	12.0
Reported predicted service life, years	6.5	11.2

Environmental and Economic Assessment

Functional unit and system boundaries

The preliminary environmental evaluation indicates that the functional unit is composed of one kilometer of paved road having 7 meters of width and 50 millimeters of surface course.

$$V = 1000 \times 7 \times 0.05 = 350\text{m}^3.$$

The mass of the mixture will be calculated based on the compacted density. The amount of modifiers will depend on the actual binder content and dosage denominator. The assessment process must differentiate between:

- **effects from cradle to placement**: material production, transport, mixing, transport, and construction; and
- **effects during the analysis period**: the initial construction and maintenance and rehabilitation explicitly modeled.

Future maintenance avoided cannot compensate for an effect inside the boundary where maintenance is excluded.

Copyright *Author (s) 2026. Distributed under Creative Commons CC BY 4.0*
Received*: 17-09-2026 -* ***Accepted****: 15-11-2026 -* ***Published****: 23-11-2026*

Status of the supplied environmental results

The stated GWP reduction is arithmetically:

$$\frac{1280 - 940}{1280} \times 100 = 26.6\%.$$

However, the final numbers will not be verifiable without the life-cycle inventory, the allocation approach for the recycled rubber, the data set for the production of graphene, transportation assumptions, the energy needed for processing, the impact assessment approach, and the maintenance plan. Thus, the observed benefit to the environment should be considered a hypothesis that needs to be confirmed through the full life cycle assessment.

Table 13. Environmental outputs.

Indicator	Unit per reported functional unit	Baseline	Modified scenario
Global warming potential	kg CO_2-eq	1,280	940
Acidification potential	kg SO_2-eq	6.0	4.4
Eutrophication potential	kg phosphate-eq	0.34	0.26
Primary energy demand	MJ	19,200	14,800

Construction and maintenance cost assumptions

The adjusted scenario indicates that the cost involved at the beginning is 30.8% more, while the annual cost of maintenance is 64.8% less. With just this information, the simple payback period would be:

$$PBP = \frac{242000 - 185000}{12800 - 4500} = 6.87 \text{ years}.$$

Therefore, the previously mentioned payback period of 4.6 years cannot be proved based solely on the above assumptions regarding construction and maintenance. Even though previous rehabilitation might influence this result, this should be evidenced explicitly.

Table 14. Supplied preliminary cost assumptions.

Cost component	Baseline	Modified scenario
Initial construction cost, USD/km	185,000	242,000
Annual maintenance cost, USD/km/year	12,800	4,500

Life-cycle cost analysis requirements

A defensible comparison should use a discounted cost framework:

$$LCC = C_0 + \sum_{t=1}^{N} \frac{C_{m,t} + C_{r,t}}{(1+r)^t} - \frac{S_N}{(1+r)^N},$$

where C_0 is initial construction cost, $C_{m,t}$ maintenance cost, $C_{r,t}$ rehabilitation cost, r the real discount rate, N the analysis period, and S_N residual value.

It is not possible to validate the 20-year totals, net present value, and benefit-cost ratio that were originally cited without the cash flow schedule. Specifically, a difference between the totals that is not discounted is not a net present value.

Practical implementation considerations

Nanomodifier implementation entails more than simply procuring the nanoscale modifier. Important factors include the quality of GNPs, dispersion on a plant scale, compatibility with rubber-binder, shelf life, production temperatures, emissions, compaction, and control of worker exposure.

It would be erroneous to assume that ultrasonication in the laboratory could be directly applied in production at the asphalt plant.

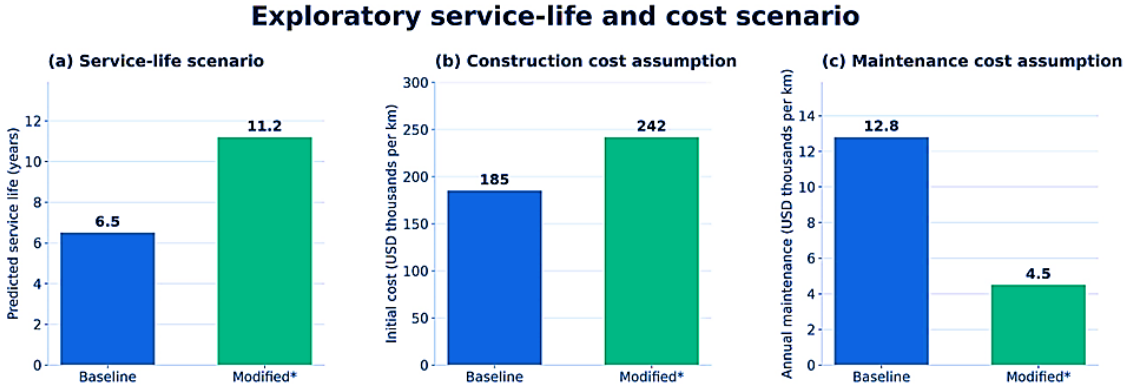

Figure 6. *Baseline and alternative estimates of the service life and costs. They are indicative scenario values and not real-world results or life-cycle cost study conclusions.*

Copyright *Author (s) 2026. Distributed under Creative Commons CC BY 4.0*
Received*: 17-09-2026 -* ***Accepted****: 15-11-2026 -* ***Published****: 23-11-2026*

Conclusion

The conclusions obtained from the description of the provided data set can be formulated as follows:

- **Composition of formulations**: The test involved six formulations. Formulation M3 contains 18% of crumb rubber and 0.1% graphene nanoplatelets (GNPs); formulation M4 contains 18% of crumb rubber and 0.3% GNPs.
- **Heat resistance**: The highest numerical value of the property under heat is demonstrated by formulation M4, with a value at 76°C that is 115.0% higher compared to formulation M0.
- **Resistance to permanent deformation and rutting**: Formulation M4 demonstrates a 63.6% decrease in permanent deformation and a 66.1% decrease in Hamburg rut depth at 70°C. Moreover, the flow number for this formulation increases from 192 to 742 cycles.
- **MSCR compatibility**: The recalculated stress sensitivity is above 75% for all formulations. Therefore, the increased compliance and recovery cannot be considered to be an evidence of M332 compatibility.
- **Balancing the properties**: The calculated TSR for formulation M4 is equal to 83.46%; the BBR stiffness is 295 MPa at −24°C. Acceptance and grading involve verification of the procedure and records used.
- **Promising dosage**: The addition of 0.3% GNP can be considered to be the most promising one among the tested rubberized asphalts; however, the statistical, chemical, and durability optimality has not been yet proven.

In general, graphene-modified rubberized asphalt needs to be further investigated as to its use on hot desert roads. The implementation of this asphalt on the roads in southern Libya will require the correction of the experiment's records and controls, adequate modeling, and pilot construction.

References

1. Polo-Mendoza, R., Navarro-Donado, T., Ortega-Martinez, D., Turbay, E., Martinez-Arguelles, G., & Peñabaena-Niebles, R. (2023). Properties and characterization techniques of graphene-modified asphalt binders. *Nanomaterials, 13*(5), 955.
2. Yang, L., Zhou, D., & Kang, Y. (2020). Rheological properties of graphene-modified asphalt binders. *Nanomaterials, 10*(11), 2197.
3. Eisa, M. S., Mohamady, A., Basiouny, M. E., Abdulhamid, A., & Kim, J. R. (2021). Laboratory evaluation of mechanical properties of modified asphalt and mixture using graphene platelets (GnPs). *Materials, 14*(19), 5599.
4. Adnan, A. M., & Wang, J. (2023). Enhancement of rheological performance and compatibility of tire rubber-modified asphalt binder with the addition of graphene. *Construction and Building Materials, 402*, 133038.
5. Almashaqbeh, H. K., Rushing, G., Doyle, J., Sengottuvelu, D., Majdoub, M., Al-Ostaz, A., Alkhateb, H., Nouranian, S., & Ucak-Astarlioglu, M. G. (2024). Effects of the geometric characteristics of graphene nanoplatelets on the physico-rheological properties of asphalt binder. *Materials and Structures, 57*, 63.
6. Li, Z., Guo, T., Chen, Y., Dong, L., Chen, Q., Hao, M., Zhao, X., & Liu, J. (2022). Study on rheological properties of graphene oxide/rubber crowd composite-modified asphalt. *Materials, 15*(18), 6185.
7. Wang, Y., Sun, Y., Huang, L., Wang, X., & Lin, C. (2026). Study on the physical properties, anti-aging properties, and rheological characteristics of graphene oxide/rubber powder composite modified asphalt. *Frontiers in Materials, 12*, 1758696.
8. Rodríguez-Alloza, A. M., & Garraín, D. (2025). Comparative life cycle assessment of rubberized warm-mix asphalt pavements: A cradle-to-gate plus maintenance approach. *Coatings, 15*(8), 899.
9. American Association of State Highway and Transportation Officials. (2023). *M 332-23: Performance-graded asphalt binder using multiple stress creep recovery (MSCR) test*. AASHTO. Official standards listing:
10. American Association of State Highway and Transportation Officials. (2023). *M 320-23: Performance-graded asphalt binder*. AASHTO. Official standards listing:
11. Moore, N., & Taylor, A. (2023). *Evaluation of IDEAL-CT testing equipment: Final report* (NCAT Report 23-02). National Center for Asphalt Technology, Auburn University.

Copyright *Author (s) 2026. Distributed under Creative Commons CC BY 4.0*
Received*: 17-09-2026 -* ***Accepted****: 15-11-2026 -* ***Published****: 23-11-2026*